ELSEVIER

Journal of Membrane Science 207 (2002) 1–16

journal of
MEMBRANE
SCIENCE

www.elsevier.com/locate/memsci

On the electrodialysis of aqueous H_2SO_4–$CuSO_4$ electrolytes with metallic impurities

L. Cifuentes [a,*], G. Crisóstomo [a], J.P. Ibáñez [a,1],
J.M. Casas [b], F. Alvarez [b], G. Cifuentes [c]

[a] Departamento de Ingeniería de Minas, Universidad de Chile, Tupper 2069, Santiago, Chile
[b] Departamento de Ingeniería Química, Universidad de Chile, Beauchef 861, Santiago, Chile
[c] Departamento de Ingeniería Metalúrgica, Universidad de Santiago, Av. B. O'Higgins 3363, Santiago, Chile

Received 18 April 2001; received in revised form 4 October 2001; accepted 17 October 2001

Abstract

This work aims to contribute to the characterization of the electrodialysis (ED) of aqueous sulfuric acid–copper sulfate solutions. The presence of impurities such as As and Sb, typical of copper electrorefining electrolytes, is also studied. Results from kinetic studies carried out in ED cells with and without re-circulation are presented. The concentrations were: 3–9 $g\,l^{-1}$ copper, 50 $g\,l^{-1}$ sulfuric acid, 3 $g\,l^{-1}$ arsenic and 0.025 $g\,l^{-1}$ antimony; the temperatures, 22 and 44 °C; the transport rates, depending on experimental conditions, 0.2–0.6 $mol\,h^{-1}\,m^{-2}$ of membrane for copper, 0.65–2.8 for sulfate, and 0.016–0.03 for arsenic. A speciation model has been developed and applied in order to interpret the experimental results and the performance of the studied cells has been evaluated. The main conclusion is that ED can be applied to the separation and concentration of chemical species in these systems. © 2002 Elsevier Science B.V. All rights reserved.

Keywords: Electrodialysis; Electrochemistry; Diffusion; Kinetics; Copper

1. Introduction

1.1. Objectives

The present work aims to study the application of electrodialysis (ED) [1–4] to the treatment of aqueous $CuSO_4$–H_2SO_4 solutions, which are the basis of copper electrometallurgy electrolytes. The latter, which also contain a range of impurities and additives, have been treated by ion exchange and other methods [5,6]. This has been done in order to separate and concentrate species, to dispose of unwanted elements and compounds and to recover valuable metals, but only one publication has dealt with the application of ED to these solutions [7]. The presence of metallic impurities such as As and Sb, typical of copper electrorefining electrolytes, is also studied. The main objective is to establish kinetic data for these systems.

The effects of current density, time, electrolyte re-circulation and species concentration on transport rates in aqueous $CuSO_4$–H_2SO_4 electrolytes have been studied in lab-scale ED cells with and without re-circulation. Additionally, experiments have been carried out with a commercially available semipilot ED cell.

Research in ED is strongly linked with work in speciation, i.e. the determination of the chemical species

---

[*] Corresponding author. Tel.: +562-678-4503; fax: +562-672-3504.
E-mail address: luicifue@cec.uchile.cl (L. Cifuentes).
[1] Present address: Department of Metallurgy, Arturo Prat University, Av. Arturo Prat 2120, Iquique, Chile.

PII: S0376-7388(01)00733-5

actually present in a given system and the distribution of their concentration as a function of pH and temperature. The aqueous speciation of the $CuSO_4$–H_2SO_4 system—with and without impurities—has been studied by several authors [8–11]. A first-approximation speciation model has been developed for the present work and applied to the interpretation of experimental results. The ED cell performance has been discussed in terms of a known expression.

Nomenclature

$\mathring{a}$	hard-core diameter (cm)
A	cross-section area perpendicular to current flow (m^2)
A_{mem}	membrane surface area (m^2)
A_{elect}	electrode surface area (m^2)
A_γ	Debye–Hückel parameter ($kg^{0.5}\,mol^{-0.5}$)
B_γ	Debye–Hückel parameter ($kg^{0.5}\,mol^{-0.5}\,cm^{-1}$)
$\dot{B}$	B-dot parameter ($kg\,mol^{-1}$)
c	concentration ($mol\,l^{-1}$)
ΔC	variation of copper concentration in the working solution during the test period ($mol\,l^{-1}$)
d	thickness of compartment (m)
D	diffusivity ($m^2\,s^{-1}$)
ΔE_e	difference between the equilibrium potentials of the anodic and cathodic reactions (V)
F	Faraday's constant ($C\,eq.^{-1}$)
G	Gas constant ($J\,mol^{-1}\,K^{-1}$)
i	applied current density ($A\,m^{-2}$)
I	cell current (A)
I_γ	ionic strength ($mol\,kg^{-1}$)
p	other undesired potential drops (V)
P_c	cation transport performance of ED cell
Q	flow rate ($l\,s^{-1}$)
R	electrical resistance (Ω)
t	time of operation (s)
T	temperature (K)
V	cell voltage (V)
V_{WS}	working solution volume (l)
W	energy requirement (J)
z	charge number
$\sum(IR)_j$	sum of potential drops in solution over all compartments (V)
$\sum(IR)_k$	sum of potential drops in membranes (V)

Greek letters

γ	activity coefficient
$\eta_a\ \eta_c$	anodic and cathodic overpotentials (V)
κ	electrical conductivity ($\Omega^{-1}\,m^{-1}$)

1.2. Previous work

Copper transport rates through cation membranes and sulfate transport rates through anion membranes have been reported in the literature for a range of experimental conditions. For instance, Picincu and Pletcher [12] studied the transport of these ions in a dialysis process, i.e. without the passage of an electric current through the cell. For 0.1 M copper in HCl and various chloride solutions, transport rates between 0.1 and 1.1 mol $h^{-1}\,m^{-2}$ of membrane were determined. These authors found that the transport rate for copper strongly depends on the Cu(II) concentration.

Lorrain et al. [13] and Elmidaoui et al. [14] studied sulfate transport through anion membranes in dialysis processes, but copper was not present in the test solutions. Chapotot et al. [15] investigated the transport of copper and other metals both in dialysis and ED processes and showed that monovalent cations are transported through cation membranes faster than divalent cations. Cation valency, size and hydration number have an influence on transport rates and the passage of a current decreases the fraction of divalent ions within the membrane phase. These authors conclude that membrane selectivity cannot be related to equilibrium parameters at the membrane–solution interphase, but to the kinetics of ion penetration into the membrane.

Chapotot et al. [16] studied the ED of 0.5 M copper sulfate in 0.5 M sulfuric acid solution with a cell current density of 500 A m^{-2} and an electrolyte flow rate of 60 l h^{-1}. In these conditions, copper transport rates ranged from 0.4 to 2.5 mol $h^{-1}\,m^{-2}$ and sulfate transport rates ranged from 10 to 16 mol $h^{-1}\,m^{-2}$ depending on the nature of the membrane. None of the cited publications dealt with cupric sulfate–sulfuric acid solutions with metallic impurities similar to those found in copper electrorefining electrolytes, which are the object of the present work.

Table 1
Initial concentrations in studied solutions

Working solution (g l^{-1})	
Cu(II)	9
H_2SO_4	50
As(III)	3
As(V)	3
Sb(III)	0.025
Anion concentrate and cation concentrate solutions (g l^{-1})	
H_2SO_4 (batch cell)	30
H_2SO_4 (re-circulation cell)	50
Anolyte and catholyte (electrode compartments) (g l^{-1})	
H_2SO_4	50

Table 2
Properties of membranes (Ionics Inc.)

Membrane	MC-3470	MA-3475
Type	Cationic	Anionic
Permselectivity (%)		
0.5 N NaCl, 1 N NaCl	96	99
Electrical resistance (Ω cm^{-2}, AC)		
0.1 N NaCl	14	17
1 N NaCl	5	8
Mullen burst strength (minimum psi)	200	200
Thermally stable	Upto 80 °C	Upto 80 °C
Chemically stable		
H_2SO_4 and HCl	Upto 30%	Upto 30%
NaOH	Upto 50%	Upto 50%
Capacity (meq. ft^{-2})	60	40
Capacity (meq. g^{-1})	1.4	1.0
Water permeability (ml h^{-1} ft^{-2} per 5 psi)	<30	<50
Thickness (mils)	16	16
Dimensional stability	Good	Good

2. Experimental

In some electrometallurgical plants spent electrolytes are disposed of after 1:4 dilution. As these diluted electrolytes could eventually be treated by ED in order to separate, concentrate and recover species according to their value, the same degree of dilution is used in this work. Typical initial concentrations of species in the studied solutions are in Table 1.

Lab-scale batch cell experiments were carried out at room temperature (22 ± 2 °C). Copper was added to the solution as Cu(II) sulfate. The membranes used in this work were Ionac MC3470 (cation) and MA3475 (anion); their characteristics are given in Table 2.

Previous to each experiment, the membranes were treated in order to liberate the sodium and chloride ions with which they are fabricated and to absorb the ions present in the solutions used in this work [17]. Membranes were treated with the solution they were meant to be in contact with during the experiments, i.e. the working solution (WS) or a sulfuric acid solution. Membranes were kept in the treating solution during 6.5 h under agitation and then left for a further 14.5 h without agitation. Then they were washed with deionized water. A rectifier was used to provide a constant current through the cell. The instrument's current range is from −2 to +2 A and the maximum cell voltage is 30 V.

Whenever As and/or Sb were used, they were dissolved from their oxides (As_2O_3, As_2O_5 and Sb_2O_3) according to the following procedure. First, the oxides were added to deionized water under agitation at 30 °C. Then, sulfuric acid (96% by weight) was slowly added. Once the desired acid concentration was obtained, the resulting solution was left under agitation during 24 h at 50 °C. Finally, the solution was filtered to remove undissolved solids. Only the lab-scale cells (with and without electrolyte re-circulation) were used to carry out the work which included As and Sb. All solutions were filtered to avoid clogging of the membranes by suspended solids.

2.1. Batch cell

A lab-scale batch ED cell was designed to carry out this work. It consisted of five compartments:

1. The central compartment contains the WS and becomes diluted with time, as cations are transported to the cathode-side compartment and anions are transported to the anode-side compartment.
2. The cathode-side compartment initially contains 30 g l^{-1} sulfuric acid and becomes concentrated in the cations present in the WS. The solution in this compartment is the cation concentrate (CC) solution.
3. The anode-side compartment initially contains 30 g l^{-1} sulfuric acid and becomes concentrated in the anions present in the WS. The solution in

this compartment is the anion concentrate (AC) solution.

4. The cathode compartment contains the cathode and the catholyte (C), whose initial composition is 50 g l^{-1} sulfuric acid. Due to the cathodic reaction (see below), the acidity of the catholyte decreases with time.
5. The anode compartment contains the anode and the anolyte (A), whose initial composition is 50 g l^{-1} sulfuric acid. Due to the anodic reaction (see below), the acidity of the anolyte increases with time.

The thickness of ED compartments (i.e. the enclosures formed by each pair of cation and anion membranes) must be small, as it affects the IR drop in solution, which means that it also increases the overall cell voltage and the energy cost of the operation. In industrial ED cells, the thickness of the compartments is of the order of 1 mm, however, the need to obtain adequate solution samples from each compartment, in order to study the cell kinetics in lab-scale cells, demands a significant volume for each individual cell. A thickness of 10 mm was chosen as a practical compromise.

Industrial cells have a low degree of agitation produced by electrolyte flow. The Reynolds number has been estimated at 100 [3]. This slight agitation was reproduced in the cell by magnetic stirring of the relevant solutions.

Acrylic was chosen as cell material because it is resistant to the chemicals involved. The cell consists of U-shaped acrylic pieces separated by rubber seals (gaskets) of 1.75 mm thickness, one at each side of the membrane. The dimensions for each compartment are: 90 mm width, 75 mm height and 10 mm depth. The anode and cathode compartments support the electrodes (48 mm width, 48 mm height, 1 mm thickness). In this work, cell current densities are referred to the apparent surface area of the electrodes. Membrane surface area was 6×10^{-3} m^2. Acrylic plates (20 mm thickness) are used at the extremes of the array, which is kept together by five stainless steel bars (6 mm diameter) bolted at both ends. The cell design is shown in Fig. 1.

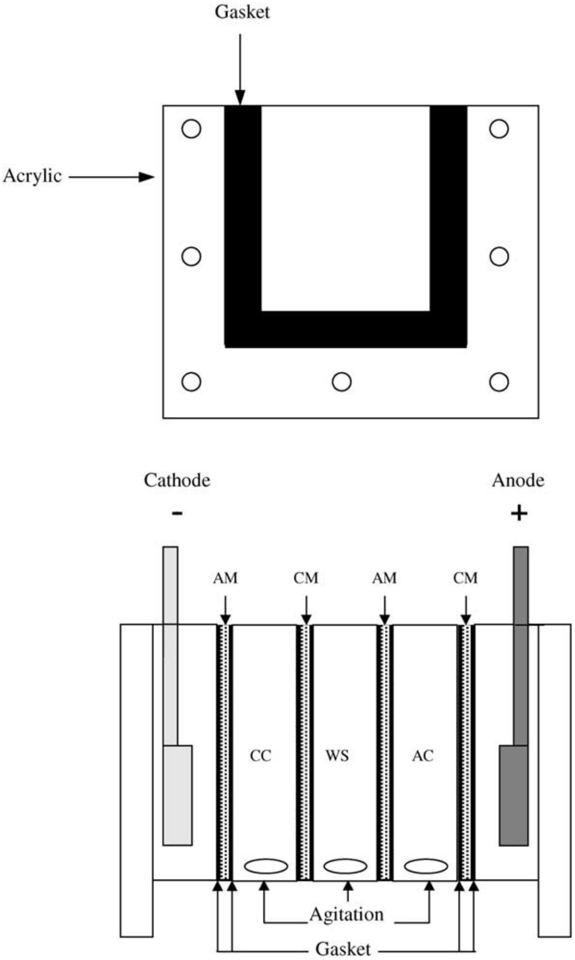

Fig. 1. Lab-scale batch electrodialysis cell: AM, anion membrane; CM, cation membrane.

The cathode was made of 304 stainless steel, which presented no problems during operation. Lead was used as anode material; in order to improve its corrosion resistance, the lead sheet was anodized in a solution which contained 150 g l^{-1} sulfuric acid and 100 ppm cobalt (from cobalt sulfate) at 50 A m^{-2} during 60 min. The reactions at the electrodes are

$$2H_2O = 4H^+ + O_2(g) + 4e, \quad \text{(anode)}$$

$$2H^+ + 2e = H_2(g), \quad \text{(cathode)}$$

The experiments lasted from 1 to 7 h and solution samples were taken at the end of every run. Concentrations were determined by atomic absorption.

Acidity was measured by titration with 0.1 M NaOH. The pH was measured with a Beckman 71 pH-meter and a Hanna combined electrode. Measurements were taken at the beginning and end of each ED run.

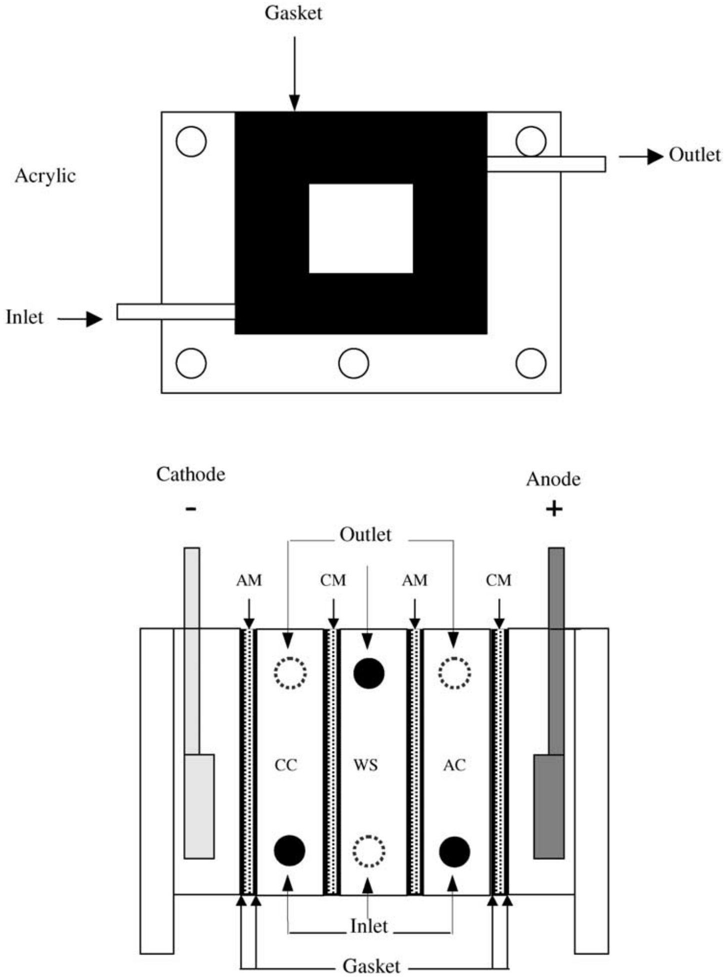

Fig. 2. Lab-scale cell with re-circulation: AM, anion membrane; CM, cation membrane.

2.2. Lab-scale cell with re-circulation

A lab-scale ED cell with re-circulation of the various electrolyte streams was designed to carry out this work. Each compartment consists of a chamber (90 mm width, 75 mm height and 10 mm depth) with 48 mm × 48 mm openings on each side to allow transport through the adjacent membranes. The anode and cathode compartments have only one 48 mm × 48 mm opening to allow transport of current through the cell. The membrane surface area was $2.2 \times 10^{-3}\,\mathrm{m}^2$. Each compartment is fitted with 4.25 mm i.d. inlet and outlet tubes to allow re-circulation, which was carried out by means of Watson Marlow 505S peristaltic pumps at a flow rate of $17\,\mathrm{l\,h}^{-1}$. Electrode dimensions and other characteristics are the same as for the batch cell. The cell design is shown in Fig. 2. The volume for all re-circulating solutions was $200\,\mathrm{cm}^3$. One liter beakers were used as re-circulation tanks.

2.3. Semipilot cell

A commercially available semipilot ED cell was used in order to study the effects of temperature and of the membrane surface area/cell volume ratio on copper and sulfate transport. The cell was a ED-1 unit (Electrosynthesis Co. Inc.). It uses a WS or feed, from which ionic species are removed, and a single concentrate solution, to which both cations and anions are transported. The membranes are separated by rubber gaskets and turbulence promoters; the set is held together by two polypropylene blocks with steel plates bolted at both ends. Four internally manifolded flow paths are provided: anolyte (anode rinse), catholyte (cathode rinse) and interleaved feed and concentrate loops. The feed or WS is depleted of ions while the concentrate solution (CONC) increases its content of both cations and anions. Four electrolyte streams (feed, concentrate, anolyte and catholyte) are driven by the peristaltic pumps mentioned above. Re-circulation tanks for each electrolyte stream are placed inside a thermostatic water bath. The volume was 500 cm^3 for all re-circulating solutions. One liter beakers were used as re-circulation tanks. Due to technical problems, the highest flow rate that could be achieved for the semipilot cell was 6 l h^{-1}.

The electrodes are 80 mm wide, 124 mm high and 1 mm thick plates made of stainless steel (anode) and platinized titanium (cathode). The 80 mm × 134 mm × 0.8 mm turbulence promoter mesh is made of high density polypropylene. The polypropylene block dimensions are 132 mm × 206 mm × 50.4 mm. The membranes are the same as in the lab-scale cell experiments, which were used after undergoing the previously described treatment. The cation and anion membranes are separated by rubber seals, leaving 0.8 mm free space between the membranes once the cell is assembled. The turbulence promoters are inserted between the membranes. For an array of three membrane pairs, the total transport surface area is 0.043 m^2 divided equally between cation and anion membranes. The electrodes were connected to the power source described above. Further details regarding this cell can be found elsewhere [18].

The experimental conditions were selected on the basis of preliminary experiments and are presented in Table 3.

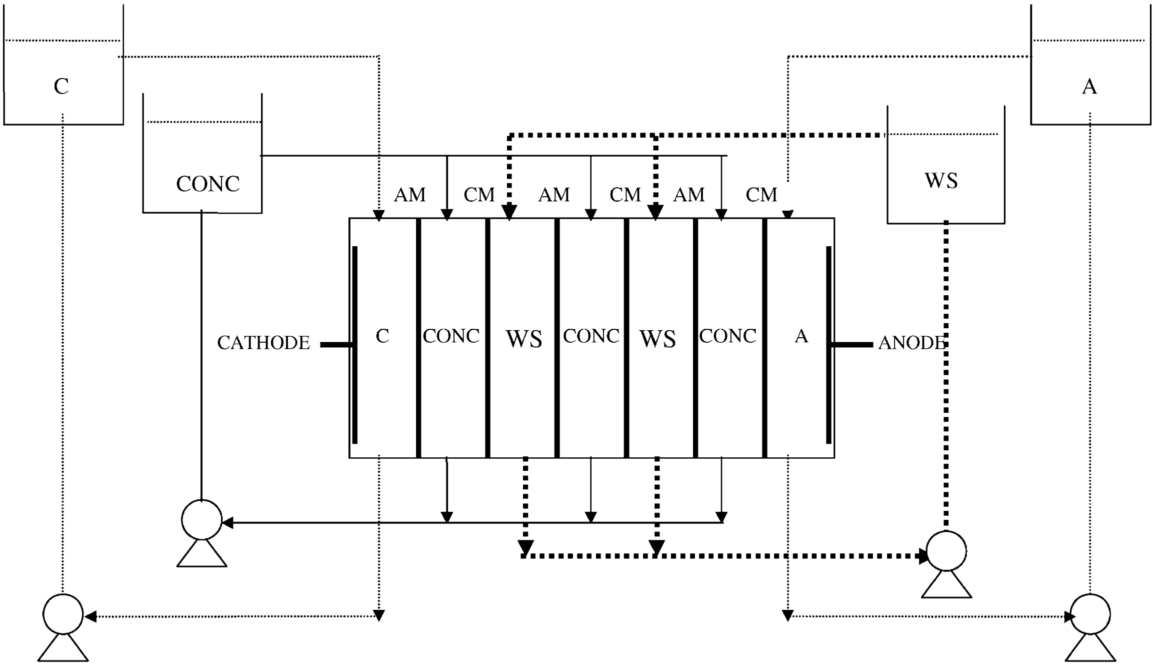

Fig. 3. Layout for the semipilot electrodialysis cell. CONC: concentrate, WS: working solution, C: catholyte, A: anolyte, AM: anion membrane, CM: cation membrane.

Table 3
Experimental conditions in semipilot cell

Initial concentration of copper (g l^{-1})	9
Concentration of sulfuric acid (g l^{-1}, all solutions)	50
Current density (A m^{-2}, referred to electrode surface area)	180
Experiment time (h)	3
Electrolyte flow rate (l h^{-1})	6
Room temperature (°C)	22 ± 2
Electrolyte volume (ml each) (catholyte, anolyte, working solution and concentrate)	500

In the experiments, one condition was changed at a time. Sulfuric acid concentration was the same in all cases. The experimental layout is schematically represented in Fig. 3. To study the effect of temperature, the re-circulation containers were placed in a Julabo thermostatic water bath unit.

3. Results

All the results gave linear dependencies, so only some of them are plotted while the rest are given as linear regression parameters in Table 4. In all cases, the concentration of the studied species (copper, sulfate, arsenic) in a given solution (working solution, cation concentrate, anion concentrate) is shown as a function of time.

Whenever the concentration is expressed as "%", it means % of the initial concentration of that species in the corresponding solution. The applied current density (A m^{-2}) is given in all cases.

3.1. Lab-scale batch ED cell

Copper transport in copper sulfate–sulfuric acid solution is presented in Fig. 4. Sulfate transport is shown

Table 4
Linear regressions for transport experiments.[a] Concentration of transported species = $A \times \text{time} + B$

Entry		I (A m^{-2})	A	B	R^2
	Batch cell				
1	Sulfate transport	225			
	SO_4^{2-} (mol%) (in WS) vs. time (h)		−4.3214	100	0.9993
	SO_4^{2-} (mol%) (in AC) vs. time (h)		4.3214	0	0.9993
2	Cu and As(III) transport	225			
	Cu (mol%) (in WS) vs. time (h)		−4.7429	99.86	0.9991
	As (mol%) (in WS) vs. time (h)		−0.8286	99.57	0.9990
	Cu (mol%) (in CC) vs. time (h)		4.7818	0	0.9990
	As (mol%) (in CC) vs. time (h)		0.9455	0	0.8640
	Re-circulation cell				
3	Transport of Cu in Cu–As–Sb–sulfate system	225			
	Cu (mol%) (in WS) vs. time (h)		−5.000	100	0.9999
	Cu (mol%) (in CC) vs. time (h)		5.000	0	0.9999
4	Transport of sulfate in Cu–As–Sb–sulfate system	225			
	SO_4^{2-} (mol%) (in WS) vs. time (h)		−6.1429	100.1	0.9993
	SO_4^{2-} (mol%) (in AC) vs. time (h)		6.0909	0	0.9992
5	Transport of arsenic in Cu–As(V)–Sb(III)–sulfate system	225			
	As (mol) (in AC) vs. time (h)		0.00006	0	0.9306
	Semipilot cell				
6	Copper transport	180			
	Cu (mol) (in CC) vs. time (h)		0.0080	0	0.9999
7	Copper transport as a function of copper concentration	180			
	Cu (mol) (in CC) vs. time (h), 9 gpl in feed		0.0080	0	0.9999
	Cu (mol) (in CC) vs. time (h), 3 gpl in feed		0.0029	0	0.9833
8	Copper transport as a function of electrolyte temperature	180			
	Cu (mol) (in CC) vs. time (h), 22 °C		0.0080	0	0.9999
	Cu (mol) (in CC) vs. time (h), 44 °C		0.0111	0	0.9969

[a] WS: working solution, CC: cation concentrate, AC: anion concentrate.

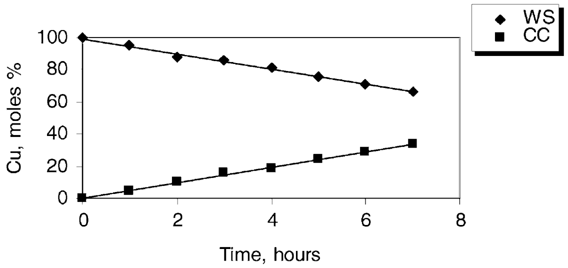

Fig. 4. Mol% of copper vs. time in working solution and cation concentrate, batch cell. Current density: $225\,\mathrm{A\,m^{-2}}$, temperature: 22 °C.

in Table 4, entry 1. The computed transport rates are $0.2\,\mathrm{mol\,h^{-1}\,m^{-2}}$ for copper and $0.65\,\mathrm{mol\,h^{-1}\,m^{-2}}$ for sulfate. In both cases, cell voltage varied between 3.9 and 4.3 V. These results show that both copper and sulfate ions can be separated and concentrated by ED.

The effect of current density on copper transport is shown in Fig. 5. Its effect on cell voltage is presented in Table 5.

The cell voltage varied within acceptable ranges at 225 and $325\,\mathrm{A\,m^{-2}}$, but it increased sharply with time at $400\,\mathrm{A\,m^{-2}}$, which indicates that the latter is not a practical proposition for the studied system.

Results for Cu and As(III) transport are presented in Table 4, entry 2. They show a clearly different behavior for these elements, with copper exhibiting a notably faster transport. After 5 h, the number of moles of copper transported from the working solution is 12.5 times higher than the amount of transported As. It must be kept in mind that the copper to arsenic initial concentration ratio is 3.6:1.

Table 5
Current density vs. cell voltage, batch cell

Current density ($\mathrm{A\,m^{-2}}$)	Cell voltage (V)
150	3.6–3.8
225	3.9–4.3
325	4.8–5.5
400	6.5–12.0

Thermodynamic calculations (see Section 4.3 and [10]) indicate that, in sulfuric solutions, both cations and anions of arsenic may be formed. In the present work, the arsenic transport rate towards the cation concentrate was $0.016\,\mathrm{mol\,h^{-1}\,m^{-2}}$, while it was not possible to quantify arsenic transport towards the anion concentrate because its concentration is within the error of the method of analysis.

As in the case of arsenic, thermodynamic calculations (see Section 4.3 and [11]) indicate that, in sulfuric solutions, both cations and anions of antimony may be formed. However, the very low solubility of Sb(III) oxide in sulfuric acid caused uncertainty in the concentrations obtained by chemical analysis, as these were mostly within the experimental error. No reliable figures can be given for Sb transport rates.

3.2. Lab-scale cell with re-circulation

Results for copper transport in the lab-scale cell with re-circulation are shown in Table 4, entry 3. When comparing results, it must be kept in mind that the solution volume in the re-circulation cell is four times

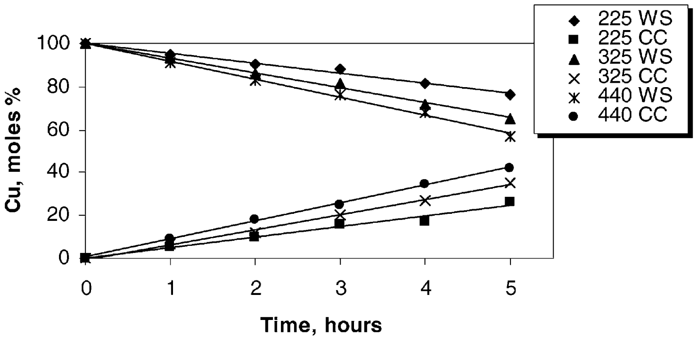

Fig. 5. Mol% of copper vs. time at various cell current densities in working solution and cation concentrate, batch cell. Temperature: 22 °C.

the solution volume in the batch cell. The Cu transport rate in the re-circulation cell is 0.61 mol h^{-1} m^{-2}, which is three times the rate in the batch cell.

Sulfate kinetics in the re-circulation cell is shown in Table 4, entry 4. The transport rate for this ion is 2.8 mol h^{-1} m^{-2}, which is more than four times the sulfate transport rate in the batch cell.

The kinetics for As(V) in the re-circulation cell are shown in Table 4, entry 5. The arsenic transport rate is very low, so the transported As is not given as percentage of the initial As concentration (relative As amount) in the working solution, but as transported moles (absolute As amount). The total transport rate for As(V) is 0.03 mol h^{-1} m^{-2}, which is twice as fast as As(III) transport in the batch cell. It is also clear that the transport rate towards the anion concentrate is consistently higher than the transport rate towards the cation concentrate, which is the opposite to what happened in the case of As(III) transport. In the case of As(V), the concentration of arsenic in the cation concentrate is within the experimental error of the analytical method, so its corresponding transport rate cannot be quantified with certainty.

Previous comments on antimony (Section 3.1) also apply here. It was detected in both the cation and anion concentrates, but no reliable figure can be given for its transport rates due to its very low solubility.

3.3. *Semipilot cell*

The experimental results for copper transport in the semipilot cell are presented in Table 4, entry 6, which represents the standard conditions (see Table 3).

Results show that the semipilot cell effectively separates copper ions. Taking into account that the cation membrane surface area is 0.022 m^2, the copper transport rate is 0.38 mol h^{-1} m^{-2}. This is nearly twice the copper transport rate in the batch cell, despite the fact that the semipilot cell was operated at 180 A m^{-2}, while the batch cell was operated at 225 A m^{-2}. The efficiencies of ED cells are discussed in Section 4.5.

The effect of the initial concentration of copper on its transport rate was investigated by carrying out an experiment at one-third of the previously studied concentration: 3 g l^{-1} of copper. Remaining conditions were as in the previous experiment. Results are presented in Table 4, entry 7. The copper transport rate decreased in roughly the same proportion as the initial concentration, which shows that copper transport is very sensitive to this variable.

Table 6
Operating conditions and cell voltage, semipilot cell

Conditions	Cell voltage (V)
9 g/l Cu, 180 A m^{-2}, 6 l h^{-1}, room temperature	3.9–4.1
[Cu] = 3 g l^{-1} Cu	3.8–4.1
$T = 44$ °C	3.7–4.0

The effect of the electrolyte temperature on the transport rate of copper was investigated by increasing the standard temperature of the electrolyte to 44.0 ± 0.2 °C. The remaining conditions were as in previous experiments. The results are given in Table 4, entry 8. A 22 °C increase in temperature caused a 38% increase in the copper transport rate (0.52 mol h^{-1} m^{-2}).

The effect of copper concentration and temperature on cell voltage is presented in Table 6. Slight cell voltage variations are measured when changing the values of copper concentration and electrolyte temperature.

3.4. *Mass balance*

A mass balance for the lab-scale cell with re-circulation, in an electrolyte which included Cu(II), As(V), Sb(III) and sulfate, is given in Table 7. The antimony balance was not included in the table due the very low solubility of Sb compounds in the studied solutions. Results are presented in moles % of the

Table 7
Mass balance in % of total amount of Cu(II), As(V) and sulfate in the re-circulation cell[a]

Species	C	CC	WS	AC	A	Total (%)
Cu i	0	0	100	0	0	100
Cu f	0	24.5	75.2	<0.5	0	<100.2
As i	0	0	100	0	0	100
As f	0	Trace	94.8	4.6	0	>99.4
$SO_4{}^{2-}$ i	14.9	21.3	27.6	21.3	14.9	100
$SO_4{}^{2-}$ f	8.0	27.2	21.0	29.4	14.4	100
pH i	0.40	0.40	0.45	0.40	0.40	
pH f	0.58	0.35	0.54	0.39	0.37	

[a] C: catholyte, CC: cation concentrate, WS: working solution, AC: anion concentrate, A: anolyte, i: initial, f: final pH values are calculated. Total amounts in working solution: Cu(II) = 9.01 g l^{-1}, S(VI) = 61.42 g l^{-1}, As(V) = 2.62 g l^{-1}, Sb(III) = 0.0038 g l^{-1}.

initial content for each component (Cu, As and sulfate) in the working solution. Copper is transported mainly towards the cathode, while sulfate and As(V) are mainly transported towards the anode. All the membranes were saturated in the solution components prior to the experiment, so further membrane adsorption is unlikely.

After 5 h operation, the concentrations of Cu, As and sulfate in the working solution decreased by 25, 5 and 6.5%, respectively. In the cation and anion concentrates, the sulfate content increased by 6 and 8%, respectively. In the catholyte and anolyte, the sulfate content decreased by 7 and 0.5%, respectively.

The calculated pH values range between 0.45 and 0.58. Proton concentration decreases in the catholyte, cation concentrate and working solution. This is caused by both proton migration towards neighboring compartments and proton reduction at the cathode. In the anolyte and anion concentrate, proton concentration increases both by proton migration from neighboring compartments and water oxidation at the anode.

The concentrations of each component over all cell compartments (Table 7) do not add up to 100% in all cases because of errors in quantitative analysis, these being <1%.

4. Discussion

4.1. Concentration versus time tests

The concentration versus time results showed that separation and concentration of Cu, As and sulfate are possible via ED. The results for Sb are inconclusive due to its very low solubility. None of the species involved seem to poison the membranes during the test period, typically 5 h. The rubber seals resisted the 50 gpl sulfuric acid electrolyte even after repeated use. The same can be said of the membranes, both anion and cation. The absolute (mol) and relative (mol%) abundances of Cu, As and sulfate, when plotted against time, produce straight lines. This linearity manifested itself in all studied cases, including the 400 A m^{-2} experiment.

It is known that in ED systems there is undesired transport of copper through anion membranes and undesired transport of sulfate through cation membranes. This is likely to occur by transport of molecular (uncharged) species or by transport of pairs of ions of opposite charge, through the membranes. In the present work, the undesired copper transport rate was of minor importance. At the end of a 5 h run in the lab-scale cell with re-circulation, copper concentration in the anion concentrate was <2% of its concentration in the cation concentrate (see Table 7).

4.2. Transport of As and Sb

4.2.1. Speciation model

In order to discuss the transport of As and Sb, it is first necessary to deal with the speciation (i.e. the distribution and concentration of dissolved species) of these elements in cupric sulfate–sulfuric acid solutions. The authors have developed a model [8,10,11] which consists of a set of equations that represent equilibrium relationships for the ionic reactions and mass balances for the components present in the system. Activity coefficients were calculated by an extended Debye–Hückel relationship as a function of temperature and ionic strength. Calculations were performed using the EQ3NR software [20]. In acidic solutions, the principal species are: HSO_4^-, H^+, Cu^{2+}, $CuSO_4$ (aq), H_3AsO_3 (aq), $H_4AsO_3^+$ and H_3AsO_4 (aq), $H_2AsO_4^-$, H_3SbO_3 (aq) and $H_2SbO_2^+$ [8,19,20].

Casas and coworkers [8,10] applied the Davies, Extended-Debye–Hückel and Pitzer models to simulate the speciation of copper and arsenic in sulfuric acid solutions. In the present work, the speciation for the H_2O–H_2SO_4–Cu–As–Sb system was calculated with the EQ3NR code using the Extended-Debye–Hückel model and an upgraded database for copper and arsenic species [10].

Ion activities are calculated with the model known as B-dot equation [20] according to the following relationship:

$$\log \gamma_i = -\frac{A_\gamma z_i^2 \sqrt{I_\gamma}}{1 + \mathring{a}_i B_\gamma \sqrt{I_\gamma}} + \dot{B} \times I_\gamma$$

where $\dot{B}$ depends only on temperature and the subindex i denotes the ith species (see list of symbols).

The speciation model is summarized in the Table 8, where reactions are represented as stoichiometric

Table 8
Stoichiometry of the main species as a function of components in the As(III)–As(V)–Cu(II)–H_2SO_4–H_2O system

Species	Components							Log *K*, at 25 °C
	H_2O	SO_4^{2-}	H^+	$H_2AsO_3^-$	$H_2AsO_4^-$	Cu^{2+}	H_3SbO_3 (aq)	
HSO_4^-	0	1	1	0	0	0	0	−1.98
$CuSO_4$ (aq)	0	1	0	0	0	1	0	−2.40
$CuHSO_4^+$	0	1	1	0	0	1	0	−2.34
H_3AsO_3 (aq)	0	0	1	1	0	0	0	−9.23
H_3AsO_4 (aq)	0	0	1	0	1	0	0	−2.27
$H_4AsO_3^+$	0	0	2	1	0	0	0	−8.94
$H_2SbO_2^+$	0	0	1	0	0	0	1	−1.49

balance equations for each defined component. The mass balance equations are as follows:

$$\mathrm{Cu(II)} = [\mathrm{Cu}^{2+}] + [\mathrm{CuSO_4(aq)}] + [\mathrm{CuHSO_4}^+]$$

$$\mathrm{As(III)} = [\mathrm{H_3AsO_3(aq)}] + [\mathrm{H_4AsO_3}^+]$$

$$\mathrm{As(V)} = [\mathrm{H_2AsO_4}^-] + [\mathrm{H_3AsO_4(aq)}]$$

$$\mathrm{Sb(III)} = [\mathrm{H_2SbO_2}^+] + [\mathrm{H_3SbO_3(aq)}]$$

$$\begin{aligned}\mathrm{SO_4(tot)} = {} & [\mathrm{SO_4}^{2-}] + [\mathrm{HSO_4}^-] + [\mathrm{CuHSO_4}^+] \\ & + [\mathrm{CuSO_4(aq)}]\end{aligned}$$

$$\begin{aligned}\mathrm{H(tot)} = {} & 2[\mathrm{H_2O}] + [\mathrm{H}^+] + [\mathrm{HSO_4}^-] + [\mathrm{CuHSO_4}^+] \\ & + 4[\mathrm{H_4AsO_3}^+] + 2([\mathrm{H_2AsO_4}^-] \\ & + [\mathrm{H_2SbO_2}^+]) + 3([\mathrm{H_3AsO_4(aq)}] \\ & + [\mathrm{H_3AsO_3(aq)}])\end{aligned}$$

Data for the equilibrium constants as functions of temperature were taken from [8,10,19,20].

4.2.2. *Model predictions*

The developed model was used to simulate the speciation in the ED experiments. The results are presented as distribution tables.

Table 9 shows the calculated speciation at 22 and 44 °C for a 0.48 m H_2SO_4, 0.14 m $CuSO_4$, 0.05 m H_3AsO_3, 0.05 m H_3AsO_4 and 0.0005 m H_3SbO_3 aqueous solution. The studied solution is highly non-ideal, due to its concentration, high acidity (pH $\approx$ 0.5) and high ionic strength (molality = 0.8). The ionic species with higher concentrations are HSO_4^-, H^+ and Cu^{2+}, and the neutral species with lower concentrations are H_3AsO_4 (aq), H_3AsO_3 (aq), H_3SbO_3 (aq) and $CuSO_4$ (aq). Copper sulfate is partially dissociated. The concentrations of SO_4^{2-} and $CuSO_4$ (aq) decrease with temperature and the concentrations of HSO_4^- and $CuHSO_4^+$ increase with temperature. Bisulfate is the main sulfate-derived species and its relative concentration increases with temperature.

The $[Cu^{2+}]/[H^+]$ concentration ratio decreases with temperature from 0.174 at 22 °C to 0.160 at 44 °C. This ratio is discussed further in Section 4.4. The stability of H^+, Cu^{2+}, $CuSO_4$ (aq), SO_4^{2-} and $H_4AsO_3^+$ decreases with temperature and the stability of HSO_4^-, $CuHSO_4^+$, H_3AsO_3 (aq), H_3AsO_4 (aq) and H_3SbO_3 (aq) increases with temperature. At

Table 9
Calculated speciation at 22 and 44 °C for an aqueous solution containing: 0.48 m H_2SO_4, 0.14 m $CuSO_4$, 0.05 m H_3AsO_3, 0.05 m H_3AsO_4 and 0.0005 m H_3SbO_3

Species	Concentration at 22 °C (mol kg^{-1} of water)	Concentration at 44 °C (mol kg^{-1} of water)
HSO_4^-	4.91×10^{-1}	5.04×10^{-1}
H^+	4.41×10^{-1}	4.03×10^{-1}
Cu^{2+}	7.68×10^{-2}	6.42×10^{-2}
SO_4^{2-}	6.56×10^{-2}	4.00×10^{-2}
H_3AsO_4 (aq)	4.89×10^{-2}	4.90×10^{-2}
$CuSO_4$ (aq)	4.57×10^{-2}	3.29×10^{-2}
H_3AsO_3 (aq)	3.94×10^{-2}	4.01×10^{-2}
$CuHSO_4^+$	1.75×10^{-2}	4.28×10^{-2}
$H_4AsO_3^+$	1.06×10^{-2}	9.86×10^{-3}
$H_2AsO_4^-$	1.15×10^{-3}	1.03×10^{-3}
$H_2SbO_2^+$	4.75×10^{-4}	4.45×10^{-4}
H_2SO_4 (aq)	1.11×10^{-4}	2.34×10^{-4}
H_3SbO_3 (aq)	2.52×10^{-5}	5.55×10^{-5}
pH	0.460	0.507
Water activity	0.980	0.981
Ionic strength	0.770	0.689

22 °C, sulfate, As(III), As(V) and Sb(III) are present mainly as HSO_4^-, H_3AsO_3 (aq), H_3AsO_4 (aq) and $H_2SbO_2^+$, respectively.

Calculations of copper speciation in the working solution and cation concentrate for batch cell experiments at 22 °C after 5 h operation indicate that copper is distributed as 55% Cu^{2+}, 32% $CuSO_4$ (aq) and 11% $CuHSO_4^+$ in the working solution. In the cation concentrate, the distribution is 60% Cu^{2+}, 30% $CuSO_4$ (aq) and 10% $CuHSO_4^+$. This is caused by different solution acidities in these solutions (see Table 1) which affect the degree of association of the relevant species.

In conclusion, the association degree of complex species in solution increases with temperature and concentration, the solutes being partially dissociated. Results from the proposed model show that the concentration of dissolved species for arsenic and copper is highly dependent on temperature, acidity and concentration. The main species, in decreasing order of concentration, are HSO_4^-, H^+, Cu^{2+}, $CuSO_4$ (aq), SO_4^{2-}, H_3AsO_3 (aq), H_3AsO_4 (aq) and $H_2SbO_2^+$. The main ionic species of As(III) and As(V) are $H_4AsO_3^+$ (or AsO^+) and $H_2AsO_4^-$ (AsO_3^-), respectively, but it must be pointed out that the concentration of ionic As species is lower than the concentration of uncharged species.

4.2.3. Direction of As and Sb transport

The direction of As and Sb transport will depend on the charge of the formed ionic species. Cations will tend to transport through the cation membrane towards the cation concentrate, while anions will tend to transport through the anion membrane towards the anion concentrate.

As(III) compounds form the $H_4AsO_3^+$ cation (also given as AsO^+) and H_3AsO_3, while As(V) compounds form the $H_2AsO_4^-$ anion and H_3AsO_4. Therefore, the expected transport direction for dissolved As(III) compounds at low pH values is through the cation membrane towards the cathode, while the expected transport direction for dissolved As(V) compounds is through the anion membrane towards the anode.

In this work, dissolved As(III) oxide gives rise to preferential transport through the cation membrane and dissolved As(V) oxide transports predominantly through the anion membrane. Both results are in agreement with theoretical predictions. In solutions where arsenic and copper ions are present, arsenic transport could be attributed to the formation of Cu–As species, but no data are available for the latter.

The speciation of antimony merits similar comments to those made regarding arsenic. Both cations and anions of Sb may form (e.g. $H_2SbO_2^+$—also given as SbO^+—and $H_2SbO_4^-$) depending on the oxidation state of the dissolved compounds. The $H_2SbO_4^-$ ion has not been included in the model presented here due to lack of thermodynamic data for Sb(V) ions. It should be kept in mind that antimony compounds are, as a rule, less soluble than arsenic ones. In solutions where arsenic and antimony coexist, the formation of As–Sb species is likely; where copper is also present, Cu–As–Sb species may form, however, to include these species in a speciation model requires further theoretical and experimental work.

In copper electrorefining electrolytes, the presence of a wide range of other impurities (e.g. Ni, Bi, Se, Te, Au, Ag, Cl) and additives (e.g. glue, thiourea) is likely to affect the speciation, thus, determining to a large extent the interaction of such solutions with membrane systems.

4.3. Effect of current density on cell voltage

The electrical resistance (R) of the electrolyte is given by

$$R = \frac{d}{\kappa A}$$

The electrical conductivity (κ) of the electrolyte is

$$\kappa = \frac{F^2}{GT}\sum c_i z_i^2 D_i$$

The overall cell voltage (V) is given by:

$$V = \Delta E_e + \eta_a + |\eta_c| + \sum (IR)_j + \sum (IR)_k + p$$

where p represents losses other than IR drops in solutions and membranes.

The cell voltage increases with increasing IR drops in solutions and membranes and it also increases with decreasing solution conductivity. The energy required by the process depends on the overall cell voltage as

$$W = VIt$$

A decrease in cell current density causes a decrease in the cell voltage, as the overpotentials of both the cathodic and anodic reactions decrease and so do the *IR* drops in electrolytes and membranes.

The results presented in Table 5, which relate to the batch cell, confirm these points: cell voltage increases slowly with cell current density up to a point where one of the compartments becomes depleted of transporting species, which causes a sharp decrease in the conductivity of the corresponding electrolyte and the cell voltage increases dramatically. In this case, the catholyte is depleted of protons causing the cell voltage to jump. This shows the importance of *IR* drops in solution, which appear to be the dominant terms in these systems.

The current densities used in this work are lower than some previously reported values (e.g. 500 A m^{-2} [16]), probably due to the low stirring degree of the working solution (batch cell) and lower flow rates in the re-circulation cells. Low agitation may cause ion depletion at the membrane surface, thus, limiting the cell current density which can be applied without a cell voltage jump.

Transport numbers for copper in various systems and conditions are presented in Table 10. They range from 0.057 to 0.145 depending on solution composition and current density. These low figures are a result of (a) the higher mobility of protons relative to cupric ions [8] and (b) the higher concentration of protons relative to cupric ions in the studied systems. Results from lab-scale batch cell experiments (runs 1–3) show that an increase in the cell current density produces a decrease in the copper transport number. This is a result of the higher mobility of protons, which migrate preferentially, thus, decreasing the current fraction available for copper transport as the cell current density increases.

Table 10
Copper transport numbers for various systems and conditions[a]

Run	System	I/A_{elect} (A m^{-2})	I/A_{mem} (A m^{-2})	t_{Cu} (%)
1	$Cu–H_2SO_4$	225	125	6.30
2	$Cu–H_2SO_4$	325	181	5.84
3	$Cu–H_2SO_4$	400	222	5.70
4	$Cu–As–H_2SO_4$	225	125	6.98
5	$Cu–As–Sb–H_2SO_4$	225	225	14.5

[a] I: cell current, A_{elect}: electrode surface area, A_{mem}: membrane surface area. Runs 1–4: batch cell, run 5: re-circulation cell, $t_{\mathrm{As(III)}}$: 0.18%.

When arsenic was added to the system, the copper transport number increased. This may be explained by the system's speciation: the addition of arsenic increases ion association, so protons tend to combine with arsenic species (e.g. with H_3AsO_3 to form $H_4AsO_3{}^+$) and proton concentration in solution decreases, which, in turn, increases the current fraction available for copper transport.

In the case of the re-circulation cell (run 5), there is a higher volume of solution in the system, so the copper concentration decrease is slower compared to runs 1 and 3. This causes a higher average copper sulfate concentration to be present during the experiment, which increases the availability of sulfate ions leading to the formation of more bisulfate and a subsequent decrease in the availability of protons. Apart from this speciation effect, which increases copper transport by migration, a higher electrolyte agitation may increase copper transport by diffusion. It must be kept in mind that the copper transport number may be interpreted as a measure of the current efficiency of the studied cells.

4.4. Effect of temperature and concentration

It was pointed out (Section 3.3) that a 22 °C increase in temperature caused nearly a 40% increase in the copper transport rate in the semipilot cell (Table 4, entry 8). The most straightforward explanation is that the solution conductivity increases with increasing ion mobilities and these, in turn, increase with temperature. Speciation calculations confirm this fact (see Tables 9 and 11).

Table 9 shows that the pH increases from 0.46 at 22 °C to 0.51 at 44 °C, which indicates a decrease in the availability of protons due to the formation of bisulfate ions. Additionally, speciation model predictions (Section 4.2.2) indicated that the $[Cu^{2+}]/[H^+]$ ratio decreases with temperature. This may be explained as follows: the degree of association of both protons and cupric ions increases with temperature (due to formation of $CuHSO_4{}^+$ in the latter case), but the association of copper ions increases more than that of protons, causing the ratio to decrease.

Table 11 shows calculated results for the $[Cu^{2+}]/[H^+]$ ratio in various systems and conditions. For the copper sulfate–sulfuric acid system, as discussed above, the ratio decreases with temperature. For the same system, as it would be expected, the ratio increases

Table 11
Calculated $[Cu^{2+}]/[H^+]$ ratio and pH as functions of concentration and temperature for an aqueous sulfuric acid solution containing Cu and As[a]

System	T (°C)	H_2SO_4 (m)	Cu(II) (m)	As(III) (m)	As(V) (m)	pH	$[Cu^{2+}]/[H^+]$
Cu–H_2SO_4	22	0.48	0.14	0.00	0.00	0.456	0.172
Cu–H_2SO_4	33	0.48	0.14	0.00	0.00	0.477	0.166
Cu–H_2SO_4	44	0.48	0.14	0.00	0.00	0.498	0.157
Cu–H_2SO_4	22	0.48	0.07	0.00	0.00	0.364	0.070
Cu–H_2SO_4	22	0.48	0.14	0.00	0.00	0.456	0.172
Cu–H_2SO_4	22	0.48	0.28	0.00	0.00	0.689	0.543
Cu–As(III)–H_2SO_4	22	0.48	0.14	0.025	0.00	0.460	0.173
Cu–As(III)–H_2SO_4	22	0.48	0.14	0.050	0.00	0.464	0.174
Cu–As(III)–H_2SO_4	22	0.48	0.14	0.100	0.00	0.473	0.177
Cu–As(III)–H_2SO_4	22	0.48	0.14	0.025	0.00	0.464	0.174
Cu–As(III)–H_2SO_4	33	0.48	0.14	0.050	0.00	0.486	0.169
Cu–As(III)–H_2SO_4	44	0.48	0.14	0.100	0.00	0.507	0.159
Cu–As(V)–H_2SO_4	22	0.48	0.14	0.00	0.025	0.455	0.172
Cu–As(V)–H_2SO_4	22	0.48	0.14	0.00	0.050	0.455	0.171
Cu–As(V)–H_2SO_4	22	0.48	0.14	0.00	0.100	0.454	0.161

[a] The basic composition is: 0.48 m H_2SO_4, 0.14 m $CuSO_4$, 0.05 m H_3AsO_3 and 0.05 m H_3AsO_4.

markedly with increasing copper concentration. The addition of As(III) causes the ratio to increase, as discussed in Section 4.3., while the addition of As(V) results in a ratio decrease. The reason for this phenomenon is that there is less association between protons and As(V) ions than between protons and As(III) ions. A deeper look at the effect of temperature on the kinetics of the studied systems would require experimental work over a wider range of temperatures.

As shown in Table 11, the $[Cu^{2+}]/[H^+]$ ratio also depends on the concentrations of metals present in solution. The value of the ratio decreases from 0.174 to 0.159 as the As(V) concentration increases from 0.025 to 0.1 M. This is caused by an acidity increase which results from the dissolution of arsenic acid. On the other hand, the ratio increases with the addition of Cu(II) or As(III) (see Table 11). This is caused by species association leading to the formation of $CuHSO_4^+$ and $H_4AsO_3^+$. At constant temperature, the ratio is mainly determined by the added amounts of $CuSO_4$ and/or H_2SO_4.

4.5. On the performance of ED cells

The cation transport performance of an ED cell may be quantified as the number of transported cation equivalents divided by the number of Faradays passed through the cell. The cell performance (P_c) is then given by the following dimensionless expression, modified from Wilson et al. [21]:

$$P_c = \frac{FQ\,\Delta C}{iA_{mem}}$$

Evaluating for the experimental conditions summarized in Table 12, the performance of the lab-scale cell with re-circulation is 4.8 times the performance of the semipilot cell.

This result reflects the ratio of the flow rates (2.8) and also the ratio of the measured copper transport rates (1.6) for the lab-scale cell and semipilot cells. The main parameter affecting cation transport performance seems to be the flowrate, as shown by Fig. 5. Comparing the 225 and 325 $A\,m^{-2}$ curves, after 3 h there is a Cu concentration difference of about 6% in the cation compartment. From this result it follows that the current density difference between the lab-scale and semipilot cells (45 $A\,m^{-2}$) could hardly explain the computed performance difference between them.

An additional consideration for the assessment of cell performance is the ratio of membrane surface area to cell volume. A higher ratio means that more membrane surface area per unit volume of working

Table 12
Comparison of cell performance, P_c ($P_c = FQ\,\Delta C/iA_{mem}$)

Parameter	Lab-scale cell (LS)	Semipilot cell (SP)	Ratio (LS/SP)
Q ($\mathrm{l\,s^{-1}}$)	4.7×10^{-3}	1.7×10^{-3}	2.8
ΔC ($\mathrm{mol\,l^{-1}}$)	20.8×10^{-3}	91.3×10^{-3}	0.23
A_{mem} ($\mathrm{m^2}$)	2.3×10^{-3}	22×10^{-3}	0.10
i ($\mathrm{A\,m^{-2}}$)	225	180	1.25
Transport rate ($\mathrm{mol\,h^{-1}\,m^{-2}}$)	0.61	0.38	1.6
Performance (P_c)	18.2	3.8	4.8

solution is available for transport. The membrane surface area (A_{mem}) available for copper transport from the working solution in the lab-scale re-circulation cell is $2.3 \times 10^{-3}\,\mathrm{m^2}$; in the semipilot cell it is $2.2 \times 10^{-2}\,\mathrm{m^2}$. The working solution volume (V_{WS}) is 0.091 l for the lab-scale cell and 0.016 l for the semipilot cell. The A_{mem} to V_{WS} ratio is $25\,\mathrm{m^{-1}}$ for the lab-scale cell and $1375\,\mathrm{m^{-1}}$ for the semipilot cell. This result shows that the semipilot cell has considerable potential as both the flow rate and cell current density could be increased, giving a much better performance.

5. Conclusions

1. It is possible to separate and concentrate Cu and As species in aqueous sulfuric acid solutions by means of ED. It is also possible to separate the sulfate ion from Cu and As species.
2. Process rate depends on cell current in a linear fashion within the studied range. The transport rate ranges, depending on experimental conditions, are 0.2–0.6 $\mathrm{mol\,h^{-1}\,m^{-2}}$ of membrane for copper, 0.65–2.8 for sulfate and 0.016–0.03 for arsenic.
3. The cell voltage increases with increasing applied current density from about 3.6 V at $150\,\mathrm{A\,m^{-2}}$ to about 5.5 V at $325\,\mathrm{A\,m^{-2}}$. An applied current density of $400\,\mathrm{A\,m^{-2}}$ produced a sharp potential increase up to 12 V in the batch cell.
4. As and Sb may form cations and anions in sulfuric acid in the studied conditions—albeit in widely different concentrations, depending on the nature of the dissolved species—so that these elements can be transported towards both the anode and the cathode. Cathodic transport for As is predominant when As is dissolved from As(III) oxide. When As(V) oxide is dissolved, anodic transport is predominant. The transport rates for antimony could not be quantified due to its very low solubility in the studied systems.
5. Copper species are transported faster than As species, which points to a separation method for Cu and As in electrolytic solutions. The transport rate ratio for Cu(II)/As(III) is 12.5 in the batch cell; it is about 20 for Cu(II)/As(V) in the lab-scale cell with re-circulation.
6. The transport number for Cu ranges between 0.057 and 0.145, depending on the cell current density and the concentrations of cupric sulfate and sulfuric acid.
7. Electrolyte re-circulation increased the transport rates significantly (three-fold for copper, four-fold for sulfate) due to increased mass transfer between solution and membrane.
8. An electrolyte temperature increase (22 °C) caused a marked increase (38%) in the copper transport rate due to an increase in ion mobilities and its effect on ion association.
9. Under the studied conditions, the lab-scale cell with re-circulation exhibited a better performance (4.8 times higher) than the semipilot cell, due to the fact that both the flowrate and the current density for the former cell were higher by factors of 2.8 and 1.25, respectively. On the other hand, the semipilot cell exhibits a membrane surface area to working solution volume ratio which is 55 times greater than the corresponding ratio for the lab-scale cell. This shows that the performance of the semipilot cell could be markedly increased.
10. Advancements in this area require further work in both the thermodynamics (speciation) and kinetics of complex $CuSO_4$–H_2SO_4–H_2O systems where impurities (including As and Sb) and

additives should be taken into account to gain a deeper understanding of the application of ED to copper electrorefining electrolytes.

Acknowledgements

This work was funded by the National Committee for Science and Technology (CONICYT, Chile) via FONDECYT project 198 0757 and FONDEF project 6F1035. Thanks are due to Iván García for his collaboration with the experimental work and to the Mining Engineering and Chemical Engineering Departments, Universidad de Chile.

References

[1] K. Rajeshwar, J. Ibanez, Environmental Electrochemistry, Academic Press, New York, 1997, pp. 432–448.

[2] H. Strathmann, Membranes and membrane separation processes, Ullmann Encyclopedia A16 (1994) 187–263.

[3] N.L. Li, Separation and Purification Technology, Marcel Dekker, New York, 1992.

[4] A. Porteous (Ed.), Desalination Technology Developments and Practice, Applied Science, London, 1982.

[5] D.B. Dreisinger, B.Y.K. Scholey, Ion exchange removal of antimony and bismuth from copper refinery electrolytes, in: W.C. Cooper, et al. (Eds.), Proceedings of the Copper'95 International Congress, Vol. III, 1995, pp. 305–314.

[6] D.B. Dreisinger, B. Leong, The Solvent Extraction and Ion Removal of As, Sb and Bi from Copper Refining Electrolytes, CANMET Report No. 0748, Ottawa, 1992.

[7] L. Cifuentes, G. Crisostomo, J.M. Casas, F. Alvarez, G. Cifuentes, The use of electrodialysis for separating and concentrating chemical species in acidic Cu–Fe–As–Sb electrolytes, in: J.E. Dutrizac, et al. (Eds.), Proceedings of the Fourth International Conference Copper'99, Vol. III (Electrorefining and Electrowinning), 1999, pp. 479–494.

[8] J.M. Casas, F. Alvarez, L. Cifuentes, On the speciation of the aqueous $CuSO_4$–H_2SO_4 system, Chem. Eng. Sci. 55 (2000) 6223–6234.

[9] J.M. Casas, F. Alvarez, L. Cifuentes, G. Crisóstomo, G. Cifuentes, Modeling the speciation of sulfuric acid–cupric sulfate solutions, in: D.B. Young, et al. (Eds.), Proceedings of the Fourth International Conference Copper'99, Vol. IV (Hydrometallurgy), 10–13 October 1999, pp. 377–399, Phoenix, AZ.

[10] J.M. Casas, J.P. Etchart, L. Cifuentes, Aqueous speciation of arsenic in sulfuric acid and cupric sulfate solutions, submitted for publication, 2001.

[11] J.P. Ibáñez, L. Cifuentes, unpublished results, 2001.

[12] L. Picincu, D. Pletcher, The transport of Cu(II) through a sulfonated styrene/divinylbenzene copolymer membrane, J. Membr. Sci. 147 (1998) 257–263.

[13] Y. Lorrain, G. Pourcelly, C. Gavach, Transport mechanism of sulfuric acid through an anion exchange membrane, Desalination 109 (1997) 231–239.

[14] A. Elmidaoui, A. Toufik Cherif, J. Molenat, C. Gavach, Transfer of H_2SO_4, Na_2SO_4 and $ZnSO_4$ by dialysis through an anion exchange membrane, Desalination 101 (1995) 39–46.

[15] A. Chapotot, G. Pourcelly, C. Gavach, Transport competition transport competition between monovalent and divalent cations through cation-exchange membranes, J. Membr. Sci. 96 (1994) 167–181.

[16] A. Chapotot, V. Lopez, A. Lindheimer, N. Aouad, C. Gavach, Electrodialysis of acid solutions with metallic divalent salts: cation-exchange membranes with improved permeability to protons, Desalination 101 (1995) 141–153.

[17] T. Sata, R. Izuo, Modification of transport properties of ion exchange membranes, XII. Ionic composition in cation exchange membranes, J. Membr. Sci. 45 (1989) 209–224.

[18] Electrosynthesis Co. Web site: http://www.electrosynthesis.com/ess/edsys.html Alternative site: http://www.scribner.com/edcell.html.

[19] R.G. Robins, Arsenic hydrometallurgy, in: R.G. Reddy, J.L. Hendrix, P.B. Queneau (Eds.), Proceedings of Arsenic Metallurgy Fundamentals and Applications, Phoenix, AZ, Warrendale, PA, 1988, pp. 215–248.

[20] T.J. Wolery, EQ3NR—A Computer Program for Geochemical Aqueous Speciation–Solubility Calculations: Theoretical Manual and User's Guide (Version 7.0), Lawrence Livermore National Laboratory, Livermore, CA, USA, 1992.

[21] J.R. Wilson, A. Cooke, W.G.B. Mandersloot, S.G. Wiechers, The electrodialysis process, in: J.R. Wilson (Ed.), Demineralization by Electrodialysis, Buttersworth, London, 1960.